

Article

The Experimental Study of an R744 Heat Pump System for an Electric Vehicle for Cabin Cooling or Heating and Battery Fast Charging Cooling †

Xilong Wang ^{1,2} , Keke Xu ², Linjie Huang ², Feng Cao ^{1,*} and Yulong Song ^{1,*}¹ School of Energy and Power Engineering, Xi'an JiaoTong University, Xi'an 710049, China² Hangzhou Sanhua Research Institute Co., Ltd., Hangzhou 310016, China

* Correspondence: fcao@mail.xjtu.edu.cn (F.C.); yulong.song@mail.xjtu.edu.cn (Y.S.)

† This paper is an extended version of our paper published, Wang, C.F.; Cao, F.; Li, M.J.; Yin, X.; Song, Y.L.; He, Y.L. Research status and future development of thermal management system for new energy vehicles under the background of carbon neutrality. *Chin. Sci. Bull.* **2021**, *66*, 4112–4128.<https://doi.org/10.1360/TB-2021-0648>. (In Chinese).

Abstract: In this paper, a new R744 heat pump system is studied. The gas cooler, evaporator, indoor heat core, and indoor gas cooler are all micro-channel heat exchangers. The R744 high pressure system adopts a combination of an accumulator and internal heat exchanger (ACCU/IHX). In addition, an electronic reversible regulating valve is added before the outdoor gas cooler, making the outdoor heat exchanger able to be used as a gas cooler or evaporator. The water-cooled condenser can improve the performance in the cooling or heating mode. The research contents contain the performance and optimal pressure under extreme conditions as a result of the experiments. The results show that the cooling capacity can reach 8.2 kW with a COP of 1.87, under a 40 °C external circulation intake. The cooling capacity on the battery side can reach 11 kW under an ambient temperature of 40 °C, which can provide a sufficient cooling capacity. Under an ambient temperature of −20 °C, the maximum heating capacity can reach 6.86 kW with a COP of 1.67. Under an ambient temperature of −15 °C, the heating capacity reaches 5.07 kW with a COP of 1.78, when the indoor air volume flow rate is 200 m³/h. Obviously, R744 heat pumps show a huge advantage, compared with the traditional PTC heating or R134a heat pumps at extremely low temperatures.

Keywords: battery fast charging cooling; CO₂ refrigerant; cooling and heating capacity

Citation: Wang, X.; Xu, K.; Huang, L.; Cao, F.; Song, Y. The Experimental Study of an R744 Heat Pump System for an Electric Vehicle for Cabin Cooling or Heating and Battery Fast Charging Cooling. *Energies* **2023**, *16*, 2061. <https://doi.org/10.3390/en16042061>

Academic Editor: Kian Jon Chua

Received: 31 December 2022

Revised: 6 February 2023

Accepted: 14 February 2023

Published: 20 February 2023



Copyright: © 2023 by the authors. Licensee MDPI, Basel, Switzerland. This article is an open access article distributed under the terms and conditions of the Creative Commons Attribution (CC BY) license (<https://creativecommons.org/licenses/by/4.0/>).

1. Introduction

After the Kigali Amendment to the Montreal Protocol, the usage of the HCFC refrigerant was reduced and eventually eliminated, because of the high global warming potential (GWP). At present, the HFC refrigerant (R134a) widely used in electrical vehicles has a very high greenhouse effect, and GWP is usually 1000~2000 times that of CO₂. Therefore, the substitution of refrigerants [1] and the improvement efficient [2] of electric vehicle heat pump systems are an urgent need for our environment.

CO₂ is a natural working medium (ODP = 0, GWP = 1) and the physical properties of CO₂ are very suitable for use as a refrigerant. The components of R744 are smaller than traditional refrigerant considering its huge latent heat in evaporating and its high volumetric refrigeration capacity. The ratio of liquid density to steam density is small. After throttling, the refrigerant is evenly distributed in each pipe. A low operating viscosity can form turbulence in the flow channel to improve the heat transfer performance. In addition, it has other noteworthy advantages, such as being non-toxic, chemically stable, non-flammable, and having an easy production.

During the subcritical cycle, because of the low discharge temperature (31.1 °C, 73.7 bar) of CO₂, it will cause the attenuation of capacity and efficiency. Lorentzen [3] proposed a transcritical cycle for automobiles in 1990. Later, Lorentzen and Petterson revived

CO₂ as a refrigerant of air conditioning systems in 1993 [4–6] and verified its feasibility, but the refrigeration effect was poor and the development was hindered. Because the range of electric vehicles is decreased at low temperatures, and there is no residual heat from the engine that can be used, and the transcritical CO₂ cycle has once again come into consideration because of its strong heating characteristics.

In recent years, scholars have carried out a lot of optimization research in order to improve the performance of CO₂ in the field of thermal management. For example, Yin [7] et al. carried out optimization research on the filling amount of a CO₂ transcritical refrigeration system under different working conditions, and proposed the concept of the filling rate. The performance of the system under the condition of under charging, appropriate charging, and overcharge showed that under charging and overcharging would cause greater attenuation to the system performance.

Scientific research institutions such as the University of Illinois [8] and the University of Maryland [9], as well as enterprises such as Sanye [10] and Nissan [11], have studied the cooling capacity of CO₂ and R134a under full ambient temperature and different driving conditions and verified that CO₂ automotive air conditioners can obtain the same cooling capacity as R134a, but their energy efficiency is slightly lower under idling, urban, and high temperature conditions. In terms of their cooling effect, in 2000, Japan's Kassonic Company released the results at the International Conference on Alternative Refrigerants for the Automotive Industry, which showed that the cooling capacity of the CO₂ passenger car air conditioning system was not lower than that of the R134a system [12]. Subsequently, R.H.H. Mager showed that the CO₂ system could provide a lower compartment temperature and shorter rapid cooling time [13]. S. Memory et al. [14] conducted a cooling experiment on a BMW 328i car. The results showed that the faster cooling time of the transcritical CO₂ air conditioning system was shortened by nearly 15 min compared with R134a. At the same time, the experimental results of A. Dragi [15] show that the air supply temperature at the evaporator side of the CO₂ system was 6 °C lower than R134a after rapid cooling. The heating characteristics of the transcritical CO₂ cycle were obviously superior to the R134a system.

In order to further promote the CO₂ heat pump air conditioning system for vehicles and make the products more compact and lightweight, Dong et al. [16] developed and used the transcritical CO₂ four-way valve, integrated gas separator regenerator, and various microchannel heat exchangers. The results show that the heating capacity of the transcritical CO₂ system was significantly improved, and still had a stable heating capacity at temperatures as low as −25 °C. At −10 °C, the heating capacity could still be increased by 80% compared with R134a. The integration scheme reduced the products in the aspect of the weight and volume, and make outstanding contributions to the industrialization of the CO₂ heat pump system.

Many scholars [17–19] have shown that there is an optimal high-pressure for transcritical CO₂ automotive air conditioners under cooling conditions, as well as control of high-pressure side pressure. In order to keep the high-pressure side pressure at the optimal value, they changed the charging amount and changed the compressor outlet pressure using back pressure valves or electronic expansion valves and other methods. Casson [20] used the differential valve to control the pressure at the high-pressure side by twice throttling. The differential valve is located at the front end of the gas–liquid separator, which is used to throttle the supercritical CO₂ gas to the saturated state. The saturated CO₂ enters the gas–liquid separator, and the expansion valve throttles the saturated liquid CO₂. This method mainly uses appropriate differential pressure at both ends of the differential valve to control the pressure to reach the optimal value.

In this study, the COP and cooling/heating capacity of the R744 system was evaluated, based on the new CO₂ heat pump system in a real structure. The main objectives of this study are as follows. One is to prove the cooling and heating capacity of R744 system under extreme conditions. The second is to show that the R744 system can meet the capacity requirement of a 10 KW battery fast charging at a high temperature. The third is to analyze

the impact of each parameter on the system energy consumption, and to provide a direction for system optimization and optimal energy consumption control.

2. Theoretical Analysis of Heat Pump Loop

The designed heat pump system can realize the function of cooling, dehumidification, and heating for a cabin. In addition, the battery side is equipped with a faster charging system. The main components include an electrical compressor, water gas cooler (WGC), inner gas cooler (IGC), outer gas cooler (OGC), BMS Chiller, EXV, accumulator with internal heat exchanger (IHX), SOV, and ERV.

The advantages of this system are as follows. The heat pump can achieve three basic functions by using three stop valves (SOV). The component of ERV makes the heat pump system simpler, which embraces the full pass and throttling function. In the cooling or heating mode, the capacity can be increased through the water-cooled condenser. In the dehumidification heating mode, the designed loop can dissipate excess heat from WGC. Finally, it has the advantages of being a direct and indirect heat pump system.

For the cooling mode (Figure 1a), the E compressor in the R744 system controls the required temperature. EXV1 is used to control the discharge pressure of the compressor in order to obtain the maximum COP. In the cooling mode, ERV is fully opened for heat dissipation by OGC. Different from the heat pump systems on the market, this heat pump system connects a water-cooled condenser between the compressor outlet and the indoor air cooler. This measure will greatly improve the heat exchange capacity and energy efficiency of the R744 system. The theoretical analysis is as follows: when the R744 heat pump is in refrigeration, the high-pressure side operates in a transcritical state, and the temperature at the high-pressure side continues to decrease, and the huge temperature slip increases the average heat transfer temperature difference between the refrigerant side and the water side. When the system needs a medium cooling capacity, the system can flexibly choose to use only the outdoor air cooler for heat dissipation, further saving the power of the passenger compartment water pump and motor water circuit.

For the dehumidification mode (Figure 1b), an indoor evaporator and outdoor heat exchanger are used as the evaporator at the same time. The indoor side evaporator can be dehumidified to ensure that the passenger compartment is not foggy. The outdoor heat exchanger is used for the evaporator to absorb more heat from the outside and disperse it to the passenger compartment side. Because this mode often operates in spring and autumn, when the heat load required by the passenger compartment is very small, even if the full-way throttle valve in front of the outdoor heat exchanger is closed, the supply power is still greater than the passenger demand, and the system can flexibly dissipate the excess heat to the outdoor low-temperature heat exchanger side, thus ensuring dehumidification and comfort in the passenger compartment.

Under a low temperature or extremely low temperature heating conditions (Figure 1c), the compressor controls the target demand air temperature, and the ERV regulates the pressure on the high-pressure side to ensure that the system operates at an optimal pressure. The heat pump systems on the market are mainly divided into indirect and direct systems. The indirect heat pump first dissipates the heat to the water side, heats the heating core through water, and the direct heat pump directly flows the refrigerant into the inner gas cooler for heating. In terms of heating speed, the direct is obviously improved compared to the indirect heat pump, but in terms of system stability, the indirect heat pump has greater advantages when the system is disturbed due to the large specific capacity and inertia at the water side. This scheme fully combines the advantages of the indirect heat pump and direct heat pump, increases the heat exchange area and quickly dissipates more heat to the passenger compartment side. During the early heating period, only the indoor air cooler is used for heating. After the outlet temperature reaches the required temperature, the indirect heating circuit is gradually opened to provide more heat to the interior of the cabin.

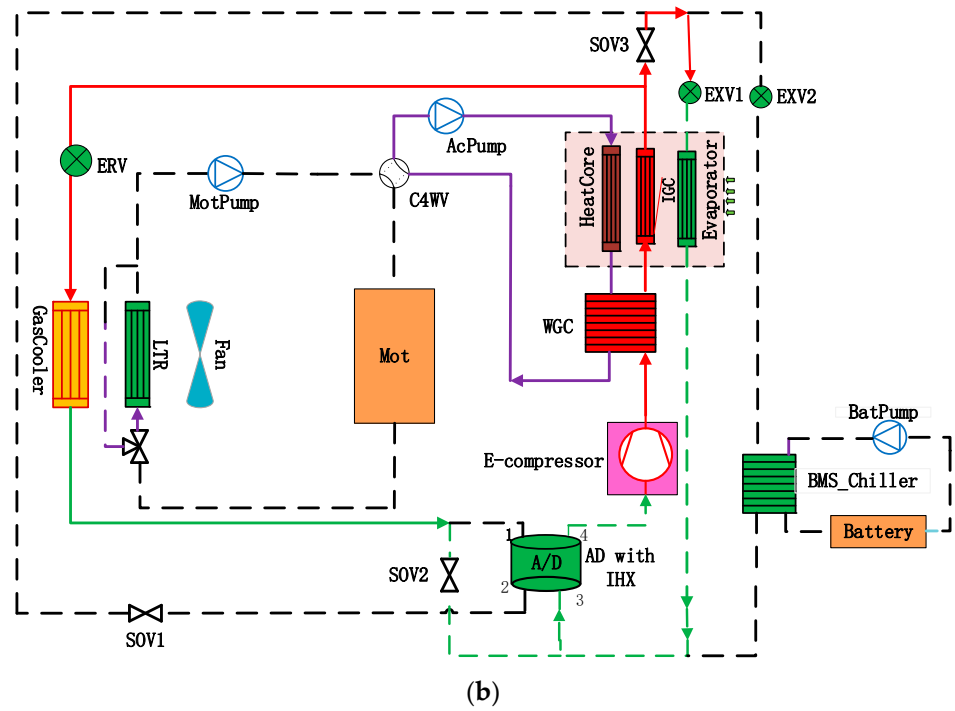
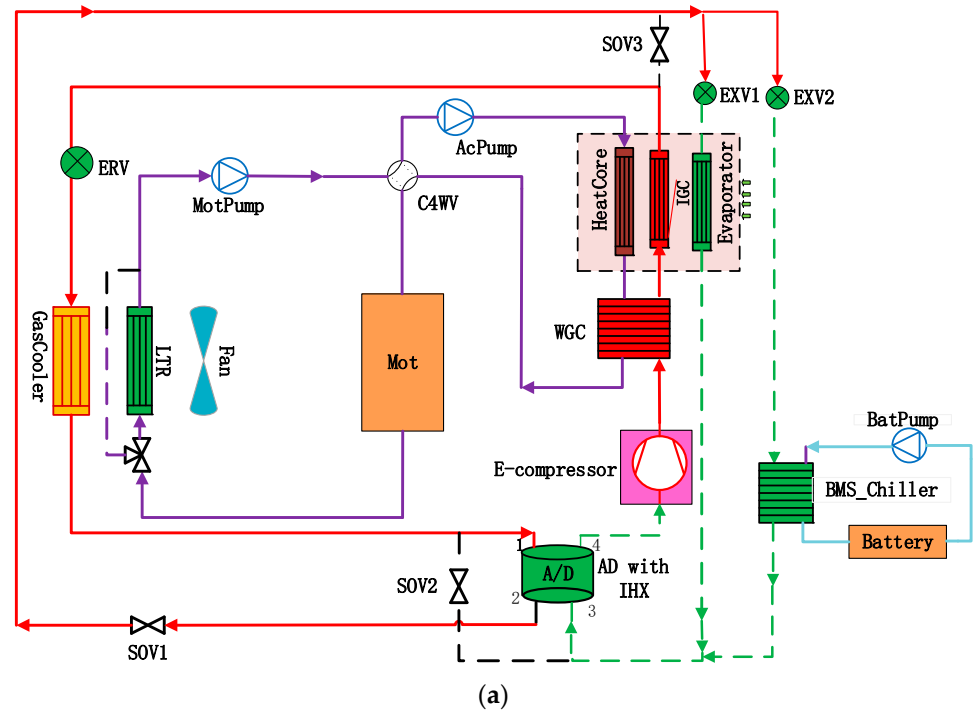


Figure 1. Cont.

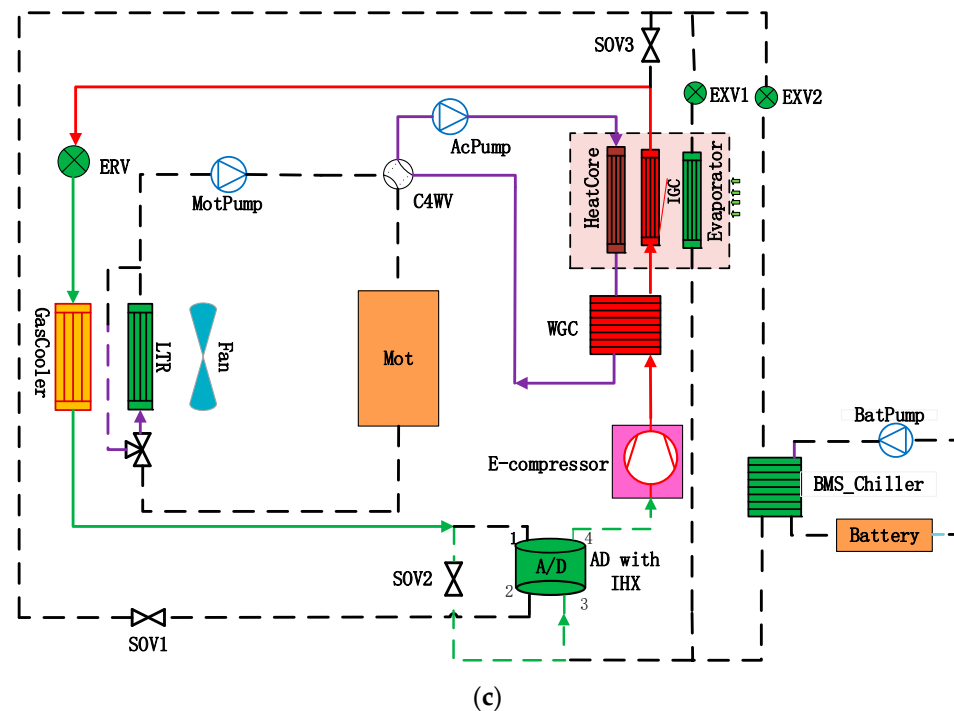


Figure 1. Schematic diagram of the R744 HP system. (a) Cooling mode, (b) dehumidification mode, and (c) heating pump mode.

3. Experimental Setup

3.1. Environmental Chambers and Wind Tunnels

A set of test benches were built according to Figure 1 and were in the research stage. During the system design, the size of the heat exchange components was configured according to the existing models on the market.

The test process was carried out in the environment chambers (Figures 2 and 3), which were divided into outdoor and indoor sides to simulate the real environment and cabin conditions. In terms of dry-bulb temperature control, the range of the two chambers could reach from 0 °C to 25 °C to 60 °C, and the accuracy was ± 0.05 °C. The control of the relative humidity was in the range from 30% to 90% based on the wet bulb temperature and the precision was $\pm 0.05\%$ at temperature above 0 °C, otherwise it was 1.7%. The air volume range in the wind tunnel indoors was 150~500 m³/h and for the outdoor tunnel it was 1500~5000 m³/h with wind resistance lower than 300 Pa.



Figure 2. Outdoor chamber.



Figure 3. Indoor chamber.

3.2. Main Components for the Systems

The heat exchangers used in the experiment had a smaller channel diameter, which was also to better for adapting to the high-pressure characteristics of R744. The combination of an accumulator and internal heat exchanger (ACCU/IHX) was installed at the suction line of the R744 HP system. The key parameters of the components in the test bench are listed in Table 1. The R744 compressor used in the experiment was also in the process of continuous optimization, which had a higher pressure and temperature bearing. In addition, its biggest feature was a small displacement because of the larger volumetric cooling/heating capacity of CO₂.

Table 1. Key characteristics of the components in the test bench.

Components of R744 HP Systems	Characteristics
Evaporator/mm	248 × 247.7 × 43.4
OHX/mm	654 × 578.3 × 12
IGC/mm	232 × 187 × 11.9
ACCU/IHX/mm	φ75.5 × 307 (IHX 37.5 × 3)
Bi-EXV	2 Ton
ERV	1 Ton
E-Compressor Disp	8.2cc
Coriolis meter	±0.5 °C FS precision
P sensor	±0.25 °C FS precision
T sensor	±0.1 °C

The T-type thermocouples were inserted into the refrigerant tube in order to reach the highest possible accuracy value. In order to obtain the refrigerant mass flow value, the compressor's outlet was equipped a Coriolis mass flow meter.

3.3. Test Data Collection and Analysis

All data were monitored through the graphical user interface software named Labview, and saved to Excel with a period of one second. By using the properties of the software REFPROP [21], the physical parameters could be easily obtained for calculation. During the experiment, we ensured the stability of the chamber and adjusted the actor until the system was stable. On the basis of stable system data, the system was run stably for another 50 min~60 min and then the 2 min test data were be extracted to find the average value.

In order to ensure the accuracy of the test data, balance calibration of the air side and refrigerant side or refrigerant side and water side were carried out at any time during the experiment. The capacity of the indoor and outdoor air side were obtained according to

the chamber. The heat exchange at the refrigerant side was equal to the multiplication of the mass flow and the enthalpy difference between the inlet and outlet. When heating or cooling the passenger compartment, we balanced and checked the data using the ratio of the heat exchange of indoor and outdoor heat exchangers to the heat exchange of the refrigerant side. During the test, the heat balance was less than 5%. In addition, the calculated data were also used as the system performance results.

The cooling capacity was calculated as follows,

$$Q_{cooling} = m_{air-in} \times h_{air-in} - m_{air-out} \times h_{air-out} \quad (1)$$

$$h = 1.005 \cdot t + d \cdot (2501 + 1.86t) \frac{\text{kJ}}{\text{kg}} (\text{dryair}) \quad (2)$$

where h is the definition of humid air enthalpy [22,23], which is the sum of 1 kg dry air enthalpy and d kg water vapor enthalpy; d is the humid air moisture content in 1 kg dry air; and m_{air-in} and $m_{air-out}$ is the dry air mass flow rate.

The heating capacity is calculated as

$$Q_{heating} = m \times c_p \times (T_{air-out} - T_{air-in}) \quad (3)$$

$$COP = \frac{Q}{W_{ecom}} \quad (4)$$

where m is the air mass flow rate, kg/h; h_{air-in} and $h_{air-out}$ are the inlet and outlet enthalpy of the air; kJ/kg; c_p is the specific heat capacity, kJ/(kg K); T_{air-in} and $T_{air-out}$ are the inlet and outlet air temperatures passing through the condenser/gas cooler, °C; W_{ecom} is the power consumed by E-Compressor, W. In cooling mode, Q is the cooling capacity, $Q_{cooling}$ and in heating mode Q is the heating capacity, $Q_{heating}$.

The total heat balance is calculated based on the gas cooler/condenser capacity and the sum of the power consumption of the compressor and the evaporator capacity. In this study, the total heat balance of the system for most test conditions is less than 5%.

The uncertainty of Q and COP is calculated as follows [24],

$$\frac{\delta Y}{Y} = \sqrt{\sum_{i=1}^n \left(\frac{\partial Y}{\partial X_i} \delta X_i \right)^2} \quad (5)$$

The maximum relative uncertainty of Q and COP in this paper is about 7.8% and 10.2%, respectively.

4. Experimental Results and Discussion for R744 HP Systems

In order to thoroughly know the features of the heat pump, the system capacity and COP of the heating and cooling were tested in low temperature and high temperature environments, respectively, and experiments were then conducted by changing the parameters to analyze the impact on the system, so we could have a comprehensive understanding of the system. At a low temperature, the experimental study was conducted at ambient temperatures of -7 °C, -15 °C, and -20 °C. At a high temperature, the refrigeration experiment was conducted at 40 °C and 35 °C. At the same time, the Chiller cooling capacity was tested at the ambient temperature of 30 °C, 40 °C, and 45 °C to verify the feasibility of the R744 refrigerant used in rapid charge cooling.

4.1. Cooling Performance of R744 HP System

In order to obtain the evaluation of the cooling performance of the R744 heat pump under an ambient high temperature, first, the indoor and outdoor air inlet temperature were 40 °C, the outdoor air inlet volume was 3 m/s, and the indoor air inlet volume was 500 m³/h. At the same time, WGC was opened, the water flow was 10 L/min, and the water inlet temperature was 52 °C. Secondly, air inlet was conducted at an ambient temperature

of 35 °C and the indoor air inlet was conducted at 27 °C to simulate the internal circulation state of the real vehicle. Finally, the cooling capacity of the chiller at various ambient temperatures was studied.

4.1.1. The Effects of Discharge Pressure on the Cooling Performance for R744 HP System at 40 °C

For the sake of obtaining the impact of discharge pressure on the system energy efficiency, the experimental research was conducted with working conditions, ambient temperature of 40 °C, indoor air inlet temperature of 40 °C, relative humidity of 40%, air inlet volume of 500 m³/h, outside gas cooler air inlet temperature of 40 °C, and air inlet speed of 3 m/s. The compressor controlled the air outlet temperature of 18 °C to achieve the same cooling capacity of 8.2 kW. By changing EXV1, the high pressure was controlled to 105 barA, 110 barA, 115 barA, and 120 barA, respectively, and the system COP was compared. The experimental results, as shown in Figure 4, indicate that when the high pressure was 110 barA, the COP value of the system energy efficiency was the highest, reaching 1.87, and it then decreased to 1.73 with the increase in high pressure. This conclusion shows the importance of optimal pressure.

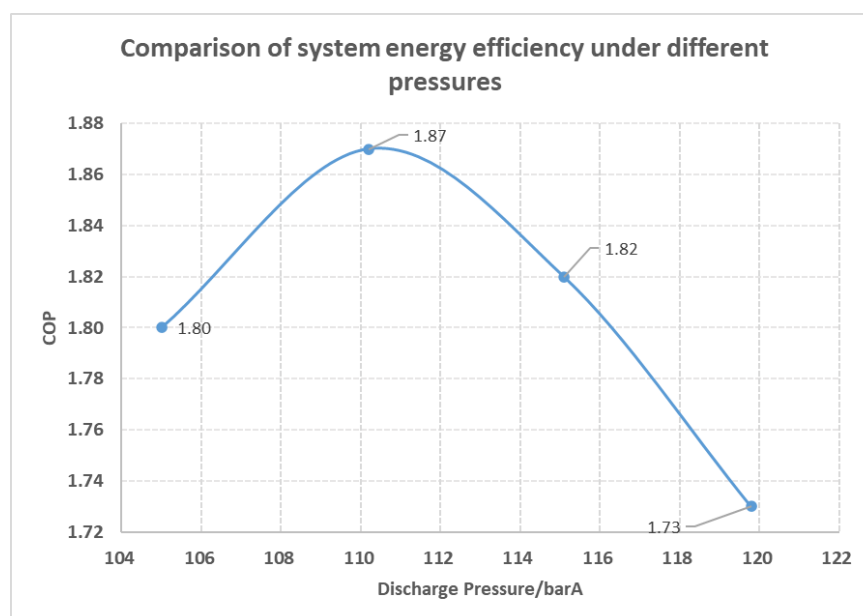


Figure 4. Change rule of COP under different discharge pressures at 40 °C.

4.1.2. The Effects of Discharge Pressure on the Cooling Performance for R744 HP System at 35 °C with an Indoor Inlet Air Temperature of 27 °C

In order to comprehend the change rule of system energy efficiency for the R744 heat pump system during the internal circulation of refrigeration, further experiments were conducted when the outdoor inlet air temperature was 35 °C, air speed was 3 m/s, indoor inlet air volume was 420 m³/h, inlet air temperature was 27 °C, and relative humidity was 40%. At the same cooling capacity of 3.4 kW, the compressor controlled the air outlet temperature at 12 °C, which means the same cooling capacity of 3.4 kW was obtained. EXV1 controlled the exhaust pressure at 85 barA, 87.5 barA, 90 barA, and 92.5 barA, respectively. The results are shown in Figure 5. When the exhaust pressure was 87.5 barA, the system COP value was the highest, reaching 2.36.

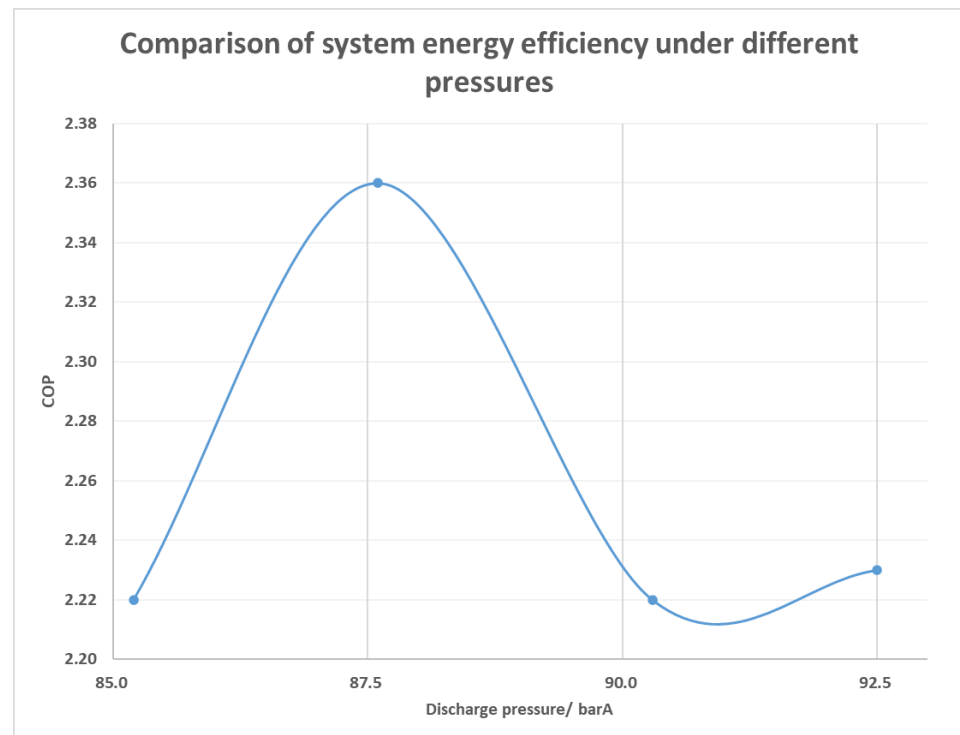


Figure 5. Variation in COP for the R744 system along with discharge pressure at 35 °C.

4.1.3. The Performance of Chiller Used for Battery Fast Cooling

In order to apply the R744 heat pump system to the battery fast charging cooling, the system cooling test was carried out at an ambient temperature of 30 °C, 40 °C, and 45 °C. The outdoor air inlet speed was uniformly 3 m/s, the water inlet flow at the chiller side was 25 L/min, and the water inlet temperature was 23.3 °C. As shown in Figure 6, when the ambient temperature was 30 °C, the compressor was 7000 rpm, the exhaust pressure was 120 barA, and the chiller cooling capacity could easily reach 13 kW; when the ambient temperature was 40 °C, the high pressure needed to be controlled at 125 barA; when the compressor was 7500 rpm, the chiller cooling capacity could reach 11 kW. When the ambient temperature was 45 °C, the high pressure was controlled at 125 barA, the compressor was 7500 rpm, and the cooling capacity of the chiller reached 9 kW.

This means that the R744 system could provide a sufficient cooling capacity when the battery was fast charged.

4.2. Heating Performance of the R744 HP System

As declared in [25], the endurance of new energy electric vehicles at low temperatures is seriously affected by the attenuation of the battery capacity and the increase in thermal load required in the passenger compartment. Moreover, conventional refrigerants, such as R134a, need a lower evaporation temperature if they are to absorb heat from the environment after being lower than the ambient temperature of −10 °C. The suction pressure is close to the atmospheric pressure, which has the risk of absorbing air. In this way, PTC heating only consumes electric energy for heating, and does not absorb heating from air. Due to the loss of heat energy, PTC heating results in efficiency less than 1 and further increases the energy consumption of the air conditioning system.

In this part, first of all, system research was carried out under an ambient temperature of −7 °C. On the premise of obtaining the same heating capacity, the change rule of the system energy consumption was studied by changing the water flow rate at the side of the heating core, different discharge pressures, different indoor air volumes, and different outdoor air volumes. Based on this rule, the maximum capacity test was carried out under

a working condition of $-7\text{ }^{\circ}\text{C}$. Then, we studied the maximum system capacity and COP at an ambient temperature of $-15\text{ }^{\circ}\text{C}$, and tested the maximum system capacity at $-20\text{ }^{\circ}\text{C}$.

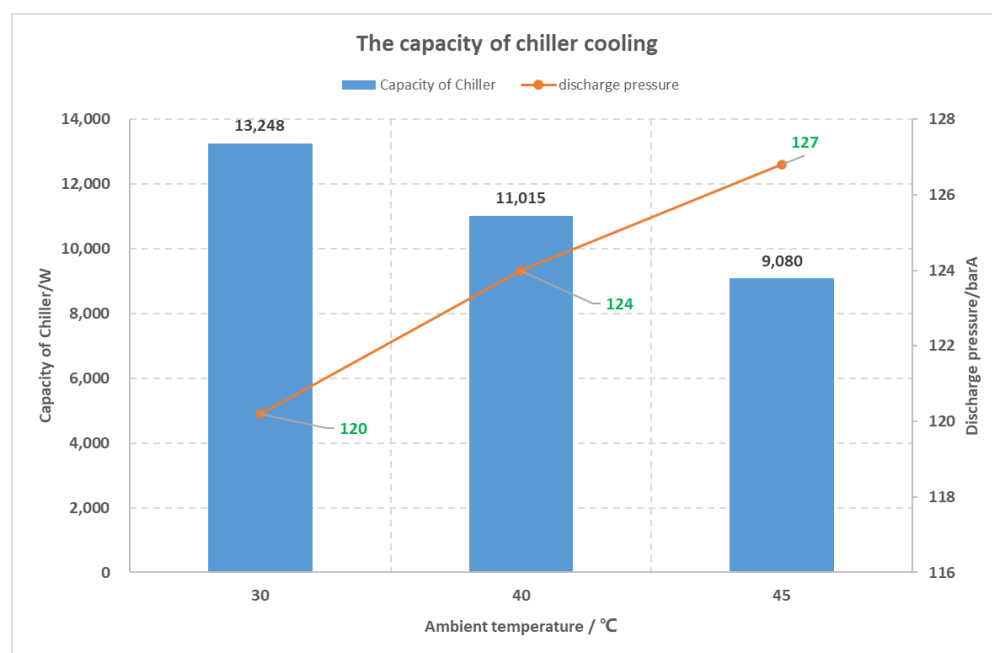


Figure 6. The capacity of chiller cooling with ambient temperatures of $30\text{ }^{\circ}\text{C}$, $40\text{ }^{\circ}\text{C}$, and $45\text{ }^{\circ}\text{C}$.

4.2.1. Heating Performance (at $-7\text{ }^{\circ}\text{C}$) Parameter Influence Experiment

In order to fully understand the influence of each variable on the R744 heat pump system, on the basis of the same heating capacity, we changed the water flow at the side of the system heating core, the air inlet speed of the outdoor heat exchanger, the air inlet volume of different HVAC, and the air outlet pressure, respectively, to obtain the change rule for the system COP.

When the indoor and outdoor air inlet temperature was $-7\text{ }^{\circ}\text{C}$, the HVAC air inlet volume was $200\text{ m}^3/\text{h}$, and the wind speed was 3 m/s , and discharge pressure of 80 barA was taken as the test pressure point. In order to reach the same air outlet temperature of $40\text{ }^{\circ}\text{C}$, we changed the water flow of the heating air core from 0 L/min to 3 L/min , 6 L/min , and obtained the system COP change rule. The experimental results in Figure 7 show that after the water flow rate increased from 0 L/min to 3 L/min , the COP value of the system had a significant increase from 1.86 to 2.04. After the water flow rate was further increased to 6 L/min , the COP value still increased, from 2.04 to 2.1, with a small increase. This shows that at 3 L/min , the heat transfer capacity of the heating air core was close to the maximum, and the capacity would not be greatly improved if the water flow increased subsequently.

Based on the influence of water flow research on the system, 3 L/min was taken as the experimental flow when the other variables below were studied.

When the indoor and outdoor air inlet temperature was $-7\text{ }^{\circ}\text{C}$, the HVAC air inlet volume was $200\text{ m}^3/\text{h}$, and the wind speed was 3 m/s , and the water flow of the heating air core was 3 L/min . In order to reach the same air outlet temperature of $40\text{ }^{\circ}\text{C}$, the discharge pressure was 80 barA , 85 barA , and 90 barA , respectively, so as to obtain the system COP change rule. The experimental results (Figure 8) show that with the increase in exhaust pressure from 80 barA to 90 barA , the COP of the system increased first and then decreased, indicating that there was an optimal COP pressure. Cause analysis: with the increase in discharge pressure, the enthalpy value at the outlet of the air cooler gradually decreased. Under the same heat exchange rate, the mass flow required by the system decreased, and the compressor speed decreased. If the enthalpy value at the outlet of the air cooler decreased more than the compressor consumption, the COP value would increase. If

the decrease in enthalpy value was far less than the increase in work consumption caused by the increase in compressor differential pressure, the COP value would decrease.

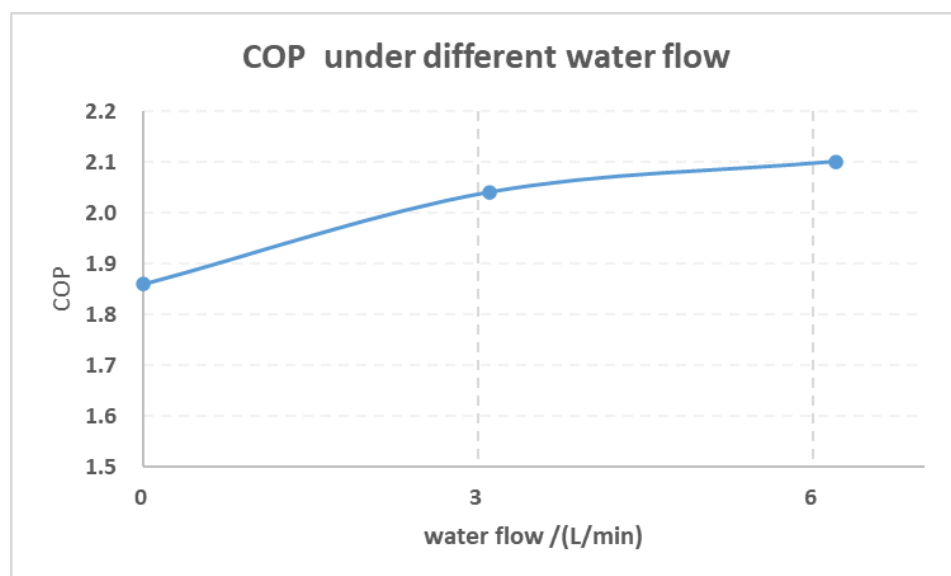


Figure 7. COP along with different water flows.

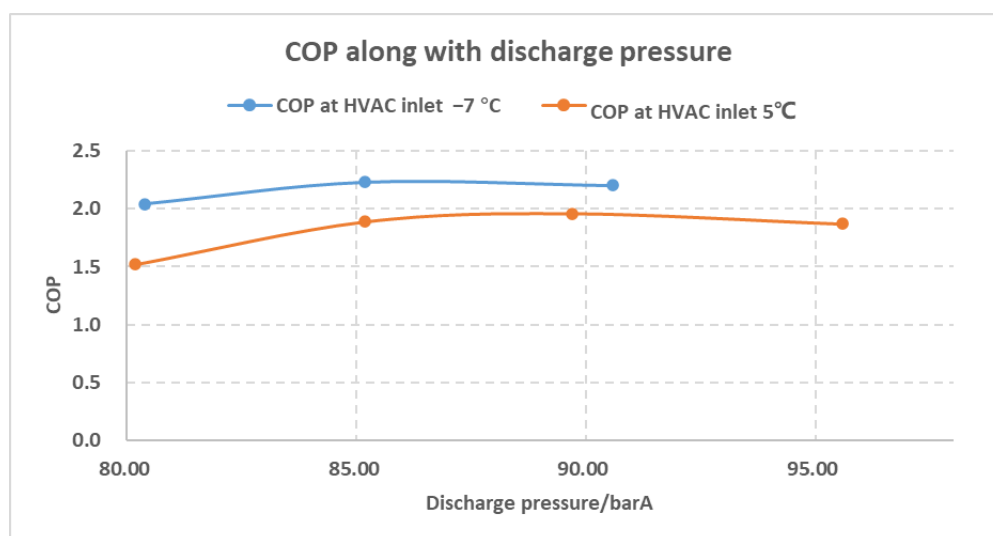


Figure 8. COP along with different discharge pressures at $-7\text{ }^{\circ}\text{C}$ and $5\text{ }^{\circ}\text{C}$.

At present, in order to improve the endurance mileage of new energy electric vehicles, most of them adopted the method of mixed vehicle interior temperature to increase the HVAC inlet air temperature. In the same way, in this experiment, research on the HVAC inlet air temperature of $5\text{ }^{\circ}\text{C}$ was carried out, and the system COP change rule was studied under the conditions of 80 barA, 85 barA, 90 barA, and 95 barA. From Figure 8, the results show that the COP of the system also showed a trend of increasing first and then decreasing with the $5\text{ }^{\circ}\text{C}$ air inlet scheme, and the maximum COP was 1.96.

By comparing the COP value of the system at the inlet air temperature of $-7\text{ }^{\circ}\text{C}$ and $5\text{ }^{\circ}\text{C}$, the COP value at $-7\text{ }^{\circ}\text{C}$ was significantly higher than that at $5\text{ }^{\circ}\text{C}$ under the same exhaust pressure. The cause analysis shows that at $-7\text{ }^{\circ}\text{C}$, the heat transfer temperature difference at the high pressure side was enhanced, and the system energy efficiency was improved. However, at the same outlet temperature, the heating capacity required for the inlet air at $5\text{ }^{\circ}\text{C}$ was significantly lower than that at $-7\text{ }^{\circ}\text{C}$.

To study the influence of different indoor air volumes on the system performance, we used $150 \text{ m}^3/\text{h}$, $200 \text{ m}^3/\text{h}$, and $250 \text{ m}^3/\text{h}$ as the air intake volumes, individually, under working conditions of indoor and outdoor air inlet temperature of $-7 \text{ }^\circ\text{C}$ and outdoor air inlet speed of 3 m/s , in order to study the relationship between the system COP and the indoor air intake volume. Because R744 has an optimal pressure when it crosses the critical value, exhaust pressures of 80 barA , 85 barA , 90 barA , and 95 barA were selected, separately, for the systematic research. The results (Figure 9) show that under the same air volume, the optimal COP value of the system increased first and then decreased with the increase in exhaust pressure. Under different indoor air intake volumes, the optimal COP value of the system was concentrated around 90 barA . This conclusion could be applied to the optimal pressure control of the whole R744 vehicle. At the same time, it also shows that under the same air outlet temperature, a large air volume could increase the system heating capacity. At this time, the COP value was large. With the increase in temperature in the vehicle, the passenger compartment demand air volume gradually decreased. At this time, the system COP value gradually decreased, and the demand heating capacity also gradually decreased.

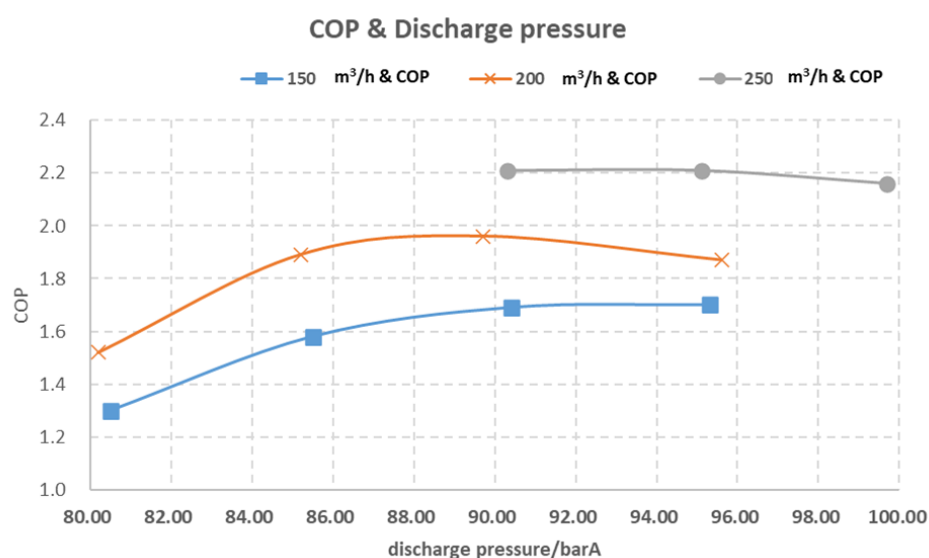


Figure 9. COP along with discharge pressures in different HVAC air flows.

In order to study the influence of the air inlet speed on the system, the relationship between the system's heating capacity and COP was studied when the indoor and outdoor air inlet temperatures were $-7 \text{ }^\circ\text{C}$, the indoor air inlet volume was $200 \text{ m}^3/\text{h}$, the water flow of the warm air core was 3 L/min , and the compressor's fixed speed was 2500 rpm . The system's high pressure was maintained at 90 barA by adjusting the ERV opening. The air inlet speed of the outdoor heat exchanger was 2 m/s , 2.5 m/s , and 3 m/s , respectively. The experimental results (Figure 10) show that, with the increase in the outdoor air inlet speed, the system heating capacity slightly increased. When the wind speed increased from 2 m/s to 3 m/s , the heating capacity increased from 3470 W to 3496 . The air outlet temperature increased from $40.2 \text{ }^\circ\text{C}$ to $40.5 \text{ }^\circ\text{C}$, and the COP value increased from 2.10 to 2.12 . The whole test results show that the change in outdoor air inlet speed had little effect on the system heating and energy efficiency.

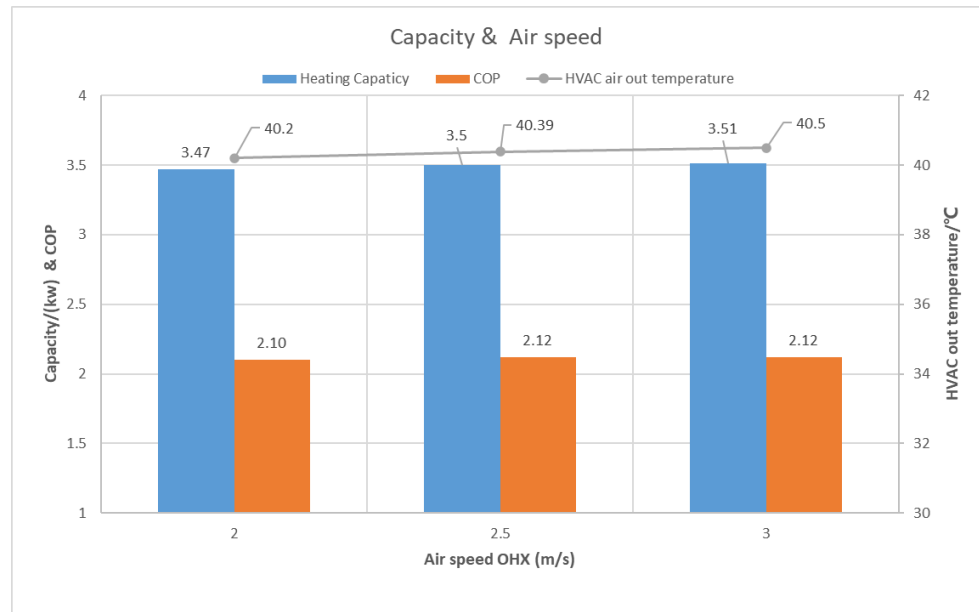


Figure 10. The capacity and air out temperature of the OHX air speed.

4.2.2. Heating Performance (−15 °C) at Different Discharge Pressures under the Same Heating Capacity

When the indoor and outdoor air inlet temperature was −15 °C at the same time, the indoor air inlet volume was 200 m³/h and the outdoor air inlet speed was 3 m/s, and the COP performance of the system under different pressures was studied under the same heating capacity, that is, the same air outlet temperature. The results show, as seen in Figure 11, that under this working condition, the R744 heat pump system could achieve a 5.07 kW heat exchange capacity, HVAC outlet air temperature of 50 °C, and system COP of 1.78. During the process of discharge pressure increasing from 85 barA to 90 barA to 95 barA, the COP of the system kept increasing, but the increasing trend was more and more slow.

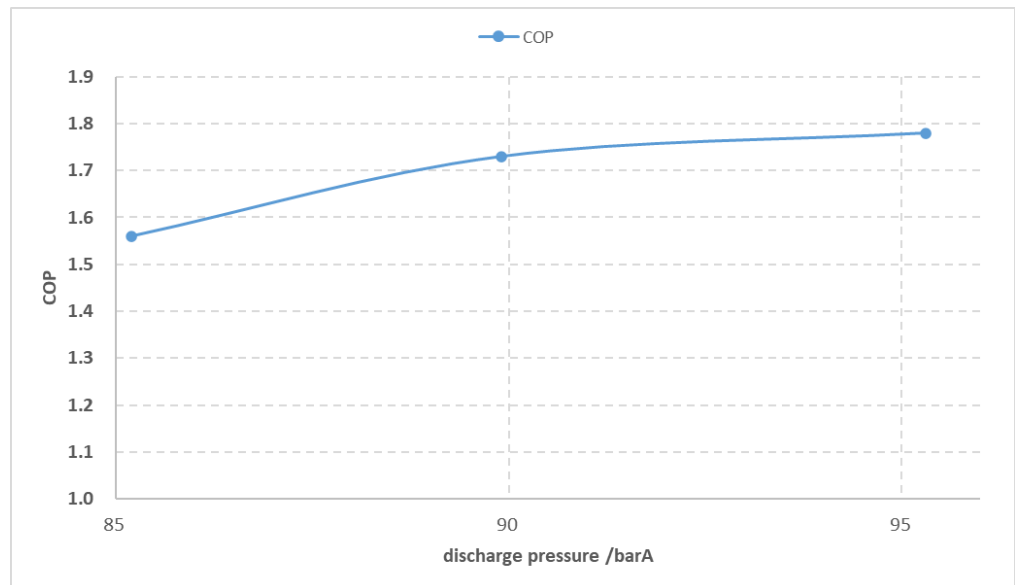


Figure 11. COP along with different discharge pressure in −15 °C.

4.2.3. Heating Performance at $-20\text{ }^{\circ}\text{C}$

Under the condition that the indoor and outdoor air inlet temperature was $-20\text{ }^{\circ}\text{C}$, the air inlet volume of the air conditioning box was $300\text{ m}^3/\text{h}$, and the outdoor air inlet speed was 3 m/s , the maximum capacity of the system was tested under the conditions that the water flow of the heating air core was 3 L/min and 6 L/min , respectively. The test results show that at $-20\text{ }^{\circ}\text{C}$, when the compressor speed was 7500 rpm , the maximum heating capacity of the system was 6.86 kW (Figure 12), the COP value was 1.67 , and the indoor air outlet temperature could reach $38.4\text{ }^{\circ}\text{C}$. At this time, the maximum capacity of the system was limited by the $135\text{ }^{\circ}\text{C}$ protection point of the exhaust temperature, and the isentropic efficiency of the compressor was only 0.57 . If the isentropic efficiency of the R744 compressor under a high-pressure difference could be improved, the heating capacity and COP of the R744 heat pump system would be further improved. When the flow rate increased from 3 L/min to 6 L/min , the heating capacity of the whole system did not increase much. This result is same as the test result when changing the water flow at ambient temperature of $-7\text{ }^{\circ}\text{C}$. The cause analysis showed that the heat exchange reached the maximum at 3 L/min when the inlet water temperature of the heating core was at a certain early stage. If more heat exchange was needed, a larger COP value could increase the HVAC air volume. Furthermore, under the working condition of $-20\text{ }^{\circ}\text{C}$ ambient temperature, the heat transfer performance of the system was not affected by increasing the water flow at the heating side, which could provide a theoretical basis for the flow control of $-20\text{ }^{\circ}\text{C}$ ambient temperature.

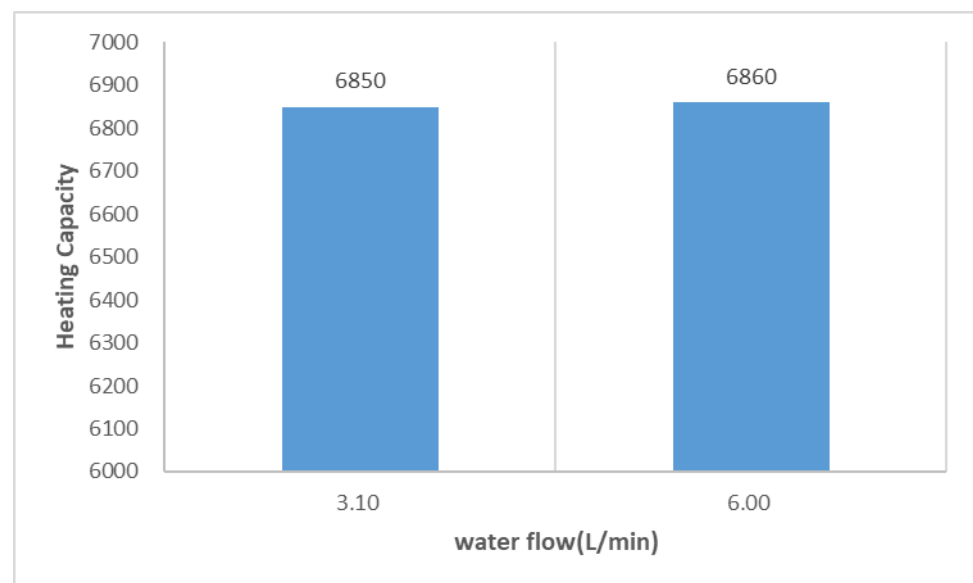


Figure 12. The heating capacity variation (in W) with different water flows.

In a word, the R744 heat pump has great potential in the for future electric vehicles, because of its considerable heating capacity and COP.

4.3. Dehumidifying Mode Performance

For the optimal COP under different operation conditions, COP was increased from 3.3 to 4.2 with the air temperature from $10\text{ }^{\circ}\text{C}$ to $4.2\text{ }^{\circ}\text{C}$, as declared in [26]. In this study, we focused on the deep performance of the system under extreme conditions that had a high energy consumption and strongly affected the vehicle range. In future work, we will study the minimum capacity between the passenger compartment and HP system under mild conditions.

5. Conclusions

This work studied the performance of the R744 heat pump system on a bench. The main purpose was to provide guidance and suggestions for vehicle thermal management design engineers and researchers. As they are needed for refrigeration or heating, the system parameters must be changed to provide system optimization and a control strategy. The main conclusions are as follows:

- (1) In the cooling mode of the R744 heat pump system, under 40 °C ambient working condition with external air circulation, the cooling capacity is 8200 W with a COP of 1.87.
- (2) Under 35 °C ambient temperature and 27 °C indoor air temperature, the COP of this system can reach 2.36.
- (3) The designed R744 heat pump system is applied to battery fast charging cooling. At 40 °C, the fast charging cooling capacity can reach 11 kW, and at 30 °C, it can reach 13 kW.
- (4) Under an ambient temperature of −20 °C, the heating capacity of the system can reach 6.85 kW, with COP of 1.67. When the ambient temperature is −15 °C and the heating capacity is 5 kW, the COP value of the system can reach 1.78. This result shows that CO₂ has an excellent performance in low temperature heating without an electric heating element compared with the traditional R134a heat pump systems.
- (5) At −7 °C, under the premise of reaching the same heating capacity, by changing the water inlet flow rate of the heating core, indoor air inlet temperature, indoor air inlet volume, outdoor air inlet speed, and other variables, the results show that at a low temperature, when the water flow rate of the heating core is 3 L/min, the system capacity can be fully utilized, and continuing to increase the water flow rate has little impact on the system energy consumption. The COP of the system heating can be improved by increasing the indoor air intake volume. However, when the heating is stable, the relationship between the volume of air and the COP of energy consumption needs to be comprehensively balanced to the volume of air considering the comfort of users. In future work, we will study the dehumidification heating function of the R744 heat pump system.

Author Contributions: Conceptualization, Y.S.; Methodology, K.X.; Validation, X.W.; Resources, L.H. and F.C.; Writing—original draft, X.W. All authors have read and agreed to the published version of the manuscript.

Funding: The authors are grateful to the National Natural Science Foundations of China (52006161) for funding this research.

Data Availability Statement: Not applicable.

Conflicts of Interest: The authors declare no conflict of interest.

References

1. Andersen, S.; Chowdhury, S.; Craig, T.; Kapoor, S.; Meena, J.; Nagarhalli, P.; Soffer, M.; Leitzel, L.; Baker, J. *Comparative manufacturing and Ownership Cost Estimates for Secondary Loop Mobile Air Conditioning Systems (SL-MACs)*; No. 2017-01-0173, SAE Technical Paper; SAE: Warrendale, PA, USA, 2017.
2. Feng, L.; Hrnjak, P. *Experimental Study of an Air Conditioning-Heat Pump System for Electric Vehicles*; SAE Technical Paper 2016-01-0257; SAE: Warrendale, PA, USA, 2016.
3. Lorentzen, G. Transcritical Vapour Compression Cycle Device. Patent WO/07683, 12 July 1990.
4. Lorentzen, G.; Pettersen, J. A new, efficient and environmentally benign system for car air conditioning. *Int. J. Refrig.* **1993**, *16*, 4–12. [[CrossRef](#)]
5. Lorentzen, G. Revival of carbon dioxide as a refrigerant. *Int. J. Refrig.* **1994**, *17*, 292–300. [[CrossRef](#)]
6. Lorentzen, G. The use of natural refrigerant: A complete solution to the CFC/HCFC predicament. *Int. J. Refrig.* **1994**, *18*, 190–197. [[CrossRef](#)]
7. Yin, X.; Wang, A.; Fang, J.; Cao, F.; Wang, X. Coupled effect of operation conditions and refrigerant charge on the performance of a transcritical CO₂ automotive air conditioning system. *Int. J. Refrig.* **2021**, *123*, 72–80. [[CrossRef](#)]
8. Boewe, D.E.; Mcenaney, R.P.; Park, Y.C.; Yin, J.M.; Bullard, C.W.; Hrojak, P.S. Comparative experimental study of subcritical R134a and transcritical R744 refrigeration systems for mobile applications. 1999. Available online: <https://www.ideals.illinois.edu/items/13405> (accessed on 30 December 2022).

9. Preissner, M.; Cutler, B.; Singanamalla, S.; Yunho, H.; Radermacher, R. Comparison of automotive air-conditioning systems operating with CO₂ and R134a. In *Science et Technique du Froid*; Institut International du Froid: Paris, France, 2001; pp. 191–198.
10. Yamamoto, K.K.S. *Experimental Evaluation of the Prototype CO₂ System and the HFC-134a System in Wind Tunnel*; Automotive Alternate Refrigerant Systems Symposiums Scottsdale: Scottsdale, AZ, USA, 1999.
11. Furuya, S.; Mathur, G. A CO₂ refrigerant system for vehicle air conditioning. In *Automotive Alternate Refrigerant Systems Symposium*; SAE: Warrendale, PA, USA, 1999.
12. Takahashi, T. Development of carbon dioxide (CO₂) applied refrigeration system. In Proceedings of the Automotive Alternate Refrigerant Systems Symposiums, Phoenix, AZ, USA, 11–13 July 2000; pp. 1–20.
13. Mager, R.H.H.; Wertenbach, J. Comparative study on AC- and HP-systems using the refrigerants R134a and R744. In Proceedings of the VDA Alternate Refrigerant Winter Meeting, Saalfelden, Austria, 30–31 January 2002.
14. Memory, S.; Verrer, F. Automotive AC/HP systems using R744 (CO₂). In Proceedings of the Sixth Vehicle Thermal Management Systems Conference (VTMS6), Brighton, UK, 18–21 May 2003.
15. Dragi, A. Carbon dioxide as the replacement for synthetic refrigerants in mobile air conditioning. *Therm. Sci.* **2008**, *12*, 55–64.
16. Dong, J.Q.; Wang, Y.B.; Jia, S.W.; Zhang, X.; Huang, L. Experimental study of R744 heat pump system for electric vehicle application. *Appl. Therm. Eng.* **2021**, *183*, 116191.
17. Inokuty, H. Graphical Method of Finding Compression Pressure of CO₂ Refrigerating Machine for Maximum Coefficient of Performance. In Proceedings of the Fifth International Congress of Refrigeration, Rome, Italy, 9–15 April 1928; pp. 185–192.
18. Boewe, D.E.; Bullard, C.W.; Yin, J.M.; Hrnjak, P.S. Contribution of Internal Heat Exchanger to Transcritical R-744 Cycle Performance. *HVAC R Res.* **2001**, *7*, 155–168. [[CrossRef](#)]
19. Hirao, T.; Mizukami, H.; Taniguchi, M. *Development of Air Conditioning System Use CO₂ for Automobile*; Purdue University: West Lafayette, IN, USA, 2000; pp. 34–36.
20. Casson, V.; Cecchinato, L.; Corradi, M.; Fornasieri, E.; Giroto, S.; Minetto, S.; Zamboni, L.; Zilio, C. Optimisation of the Throttling System in a CO₂ Refrigerating Machine. *Int. J. Refrig.* **2003**, *26*, 926–935. [[CrossRef](#)]
21. REFPROP. *Thermodynamic Properties of Refrigerants and Refrigerant Mixtures, Version 9.0*; National Institute of Standards and Technology: Gaithersburg, MD, USA, 2010.
22. ANSI/ASHRAE Standard 33-2000; Methods of Testing Forced-Circulation Air-Cooling and Air-Heating Coils. American Society of Heating, Refrigerating and Air-Conditioning Engineers, Inc.: Atlanta, GA, USA, 2000.
23. Chinese GB/T 7725-2004; No-Ducted Air Conditioners and Heat Pumps—Testing and Rating for Performance. Standards Press of China: Beijing, China, 2004.
24. Moffat, R.J. Describing the uncertainties in experimental results. *Exp. Therm. Fluid Sci.* **1988**, *1*, 3–17. [[CrossRef](#)]
25. He, L.; Jing, H.; Zhang, Y.; Li, P.; Gu, Z. Review of thermal management system for battery electric vehicle. *J. Energy Storage* **2023**, *59*, 106443. [[CrossRef](#)]
26. Wang, A.; Cao, F.; Yin, X.; Jia, F.; Fang, J.; Wang, X. Pseudo-optimal discharge pressure analysis of transcritical CO₂ electric vehicle heat pumps due to temperature glide. *Appl. Therm. Eng.* **2022**, *215*, 118856. [[CrossRef](#)]

Disclaimer/Publisher’s Note: The statements, opinions and data contained in all publications are solely those of the individual author(s) and contributor(s) and not of MDPI and/or the editor(s). MDPI and/or the editor(s) disclaim responsibility for any injury to people or property resulting from any ideas, methods, instructions or products referred to in the content.